Optimal quantum control in nanostructures: Theory and application to a generic three-level system

Alfio Borzì and Georg Stadler
Institut für Mathematik, Karl-Franzens-Universität Graz, Heinrichstraße 36, 8010 Graz, Austria

Ulrich Hohenester*
Institut für Theoretische Physik, Karl-Franzens-Universität Graz, Universitätsplatz 5, 8010 Graz, Austria
(Received 26 June 2002; published 21 November 2002)

Coherent carrier control in quantum nanostructures is studied within the framework of *optimal control*. We develop a general solution scheme for the optimization of an external control (e.g., lasers pulses), which allows to channel the system's wave function between two given states in its most efficient way; physically motivated constraints, such as limited laser resources or population suppression of certain states, can be accounted for through a general cost functional. Using a generic three-level scheme for the quantum system, we demonstrate the applicability of our approach and identify the pertinent calculation and convergence parameters.

DOI: 10.1103/PhysRevA.66.053811 PACS number(s): 42.50.Ct, 42.50.Hz, 02.60.Pn, 78.67.−n

I. INTRODUCTION

Recent years have witnessed enormous interest in controlling quantum phenomena in a variety of nanoscale systems [1]. Quite generally, such a control allows us to modify the system's wave function at will through appropriate tailoring of external fields, e.g., laser pulses: While in *quantum optics* the primary interest of this wave-function engineering lies in the exploitation of quantum coherence among a few atomic levels [2], in *quantum chemistry* optical control of molecular states has even led to the demonstration of optically driven chemical reactions of complex molecules [3]; furthermore, starting with the seminal work of Heberle *et al.* [4], coherent-carrier control in semiconductors and semiconductor nanostructures has recently been established as a mature field of research on its own. In particular, with the advent of semiconductor quantum dots [5], sometimes referred to as *artificial atoms*, one now has a system at hand which resembles many of the atomic properties whilst offering at the same time all the flexibility of semiconductor nanostructures; experimentally basic quantum-coherence phenomena such as polarization beating [6] or Rabi-type flopping [7] have been demonstrated, whereas theoretical effects such as coherent population transfer [8,9] or entanglement control [10–12] have been proposed.

In the last few years this research area has received further impetus from the emerging fields of quantum computation and quantum communication [13], aiming at quantum devices where the wave function can be manipulated with highest possible precision (*quantum gates*). This high-fidelity quantum-state engineering calls for strategies that allow an optimal suppression of environment losses during gating; self-evidently, such an outstanding performance can only be achieved if the most sophisticated experimental and theoretical techniques for optical control of quantum nanostructures are put together. It is worth emphasizing that hitherto there exists no clear consensus on how to optimally tailor the system's control, and it appears that each field of research has come up with its own strategies. For instance, quantum-optical implementations in atoms benefit from the long atomic coherence times of metastable states, and it usually suffices to rely on effective models that can be grasped from the solution of simplified level schemes (e.g., adiabatic population transfer in an effective three-level system [14]); in contrast, in quantum chemistry the complexity of molecular states usually does not permit schemes that are solely backed by the underlying level schemes, and learning algorithms that receive direct feedback from experiment, appear to be the method of choice. Finally, coherent control in semiconductor nanostructures has hitherto been primarily inspired by quantum-optical techniques; however, it is clear that control in future quantum devices will require more sophisticated techniques to account for the enhanced dephasing in the solid states; a first step in this direction has been undertaken in Refs. [11,12], where the authors have adopted control techniques developed in nuclear-magnetic resonance [15] to semiconductor nanostructures.

In this paper, we examine the problem of coherent-carrier control in quantum nanostructures within the framework of *optimal control* [16–19]. Here, one starts by defining the *optimality criteria* (the cost functional); in general, for a desired quantum-state transition, this functional will depend on the final state, the wish to suppress the population of certain states during the control process, as well as other physically motivated constraints, e.g., limited laser resources. The grand strategy then is to minimize this cost functional and to find the optimal time dependence of the control fields, which, in turn, governs the evolution of quantum states through the underlying dynamic equations (i.e., Schrödinger or master equation). The calculation of the necessary optimality conditions for this optimization problem results in a system of coupled equations, which, for high-dimensional systems, may involve heavy computations. Yet, the clear-cut advantage of this optimization approach is the flexibility to steer

*Electronic address: ulrich.hohenester@uni-graz.at

the control strategies through modification of the cost functional, thus rendering this technique ideal for the purpose of quantum-state engineering.

We have organized our paper as follows. Our theoretical approach is presented in Sec. II; in Sec. III, we derive the numerical algorithm for the solution of the relevant equations. As a first example, in Sec. IV, we study the optimal control of a generic three-level system. Section V summarizes our numerical results, and we finally draw some conclusions in Sec. VI.

II. THEORY

Consider the Schrödinger equation for a n-component wave function $\psi \in L^2(\mathbb{C}^n,[0,T])$:

$$i\dot{\psi}=H\psi, \quad \psi(0)=\psi_0, \tag{1}$$

where the Hamiltonian $H=H_0+H_\epsilon$ accounts for the unperturbed system H_0, and the coupling H_ϵ, to an external control field ϵ, where

$$||H_{\epsilon(t)}|| \leqslant K||\epsilon(t)||, \quad K>0 \tag{2}$$

is supposed to hold for all $t\in[0,T]$; finally, ψ_0 is the initial state of the system ($\hbar=1$ throughout). Note that, strictly speaking, the wave-function description of Eq. (1) is only allowed for an isolated quantum system. For the problem of our present concern (control in presence of dephasing and relaxation), a more general *density-matrix description* would be required [2] to account for the incoherent environment couplings. However, following the procedure outlined in Ref. [20], we observe that even in presence of such coupling it is possible to define a non-Hermitian Hamiltonian of the form (1), accounting for the dephasing and generalized outscatterings, if, at the same time, one introduces a further term that accounts for generalized inscatterings. Thus, since we are aiming at an optimal control of the *coherent* time evolution, i.e., we are seeking for solutions that minimize environment losses (see also Sec. IV), we can safely neglect inscattering terms, and we are led to Eq. (1), with H_0 being non-Hermitian.

In the following, we shall consider the problem of determining the control fields $\epsilon\in L^2(\mathbb{C},[0,T])$, such that Eq. (1) is fulfilled. In so doing we shall be guided by a number of further constraints, which, all together, form the so-called *optimal criteria*: first, we assert that the control sequence brings the system at time T to the desired state $\psi_d\in\mathbb{C}^n$; second, we account for the limited laser resources through a minimization of the control field strengths; third, we may wish to suppress the population of intermediate states that suffer strong environment losses (see discussion below). More specifically, all these constraints are summarized in the cost functional:

$$J(\psi,\epsilon) := \frac{1}{2}|\psi(T)-\psi_d|^2_{\mathbb{C}^n} + \frac{\gamma}{2}||\epsilon||^2_{L^2(\mathbb{C},[0,T])} + \frac{1}{2}\sum_{j=1}^{n}\alpha_j||\psi_j||^2_{L^2(\mathbb{C},[0,T])}, \tag{3}$$

where the constants $\gamma>0, \alpha_i\geqslant 0$ are the weighting factors, which allow to vary the relative importance of the various terms, and $\psi_j\in L^2(\mathbb{C},[0,T])$ denotes the jth component of ψ; the last term of Eq. (3) penalizes the occupation of certain components ψ_j during the control process. Apparently, further constraints could be added in a completely similar fashion. The optimal control problem under consideration can now shortly be written as

$$\min J(\psi,\epsilon) \quad \text{subject to Eq. (1).} \tag{4}$$

We now state that Eq. (4) has a solution.

Theorem 1. The optimal-control problem (4) *admits a solution* $(\overline{\psi},\overline{\epsilon})\in H^1(\mathbb{C}^n,[0,T])\times L^2(\mathbb{C},[0,T])$.

Proof. The above theorem can be verified in a completely analogous fashion to Ref. [18], which we omit for the sake of brevity (see also Ref. [19] for mathematical details). ■

To calculate the necessary optimality conditions of first order for Eq. (4), we use the method of Lagrange multipliers [16] to turn the constrained minimization problem (4) into an unconstrained one. For this purpose, we define the Lagrangian function

$$L(\psi,p,\epsilon)=J(\psi,\epsilon)+\mathrm{Re}\langle p, i\dot{\psi}-(H_0+H_\epsilon)\psi\rangle.$$

Here, $\langle\phi,\psi\rangle=\int_0^T\phi\cdot\psi^* dt$, where "*" means complex conjugate and the dot "$\cdot$" denotes the usual vector-scalar product in $\mathbb{C}^n$.

Consider the minimization problem: Find $\tilde{\psi}$, $\tilde{p}$, and $\tilde{\epsilon}$ such that

$$L(\tilde{\psi},\tilde{p},\tilde{\epsilon})=\inf_{\psi\in X_t^0, p\in X_t, \epsilon\in X_t} L(\psi,p,\epsilon),$$

where $X_t=L^2(\mathbb{C}^n,[0,T])$ and $X_t^0=X_t\cap\{\psi:\psi(0)=\psi_0\}$. Here, the necessary conditions for a minimum are obtained by equating to zero the Fréchet derivatives of L with respect to the triple (ψ,p,ϵ). The following optimality system is obtained:

$$i\dot{\psi}=(H_0+H_\epsilon)\psi \text{ with } \psi(0)=\psi_0, \tag{5a}$$

$$i\dot{p}=(H_0^*+H_\epsilon)p-q \text{ with } ip(T)=\psi(T)-\psi_d, \tag{5b}$$

$$\epsilon=\frac{1}{\gamma}\mathrm{Re}\left[p\cdot\left(\frac{\partial H}{\partial\epsilon_r}\psi\right)^*\right]+i\frac{1}{\gamma}\mathrm{Re}\left[p\cdot\left(\frac{\partial H}{\partial\epsilon_i}\psi\right)^*\right], \tag{5c}$$

where $q_j=\alpha_j\psi_j$ and $\epsilon=\epsilon_r+i\epsilon_i$. Notice that while the state equation (5a) evolves forward in time, the adjoint equation (5b) is marching backwards. The control equation (5c) provides the control function.

III. NUMERICAL ALGORITHM

In this section, we formulate a numerical algorithm that solves the optimality system (5a)–(5c) for given initial and final configurations ψ_0 and ψ_d, respectively. To solve this problem, we apply a gradient-type minimization algorithm that first determines a search direction with respect to the variable ϵ for both the real and imaginary parts. Then, a

simple step-size procedure is applied that guarantees a decrease in the cost functional. For given ϵ, the search direction is calculated as follows: the initial condition for the state equation is given by ψ_0. Once the wave function at $t=T$ is computed, the final condition for the adjoint equation is given by $ip(T)=\psi(T)-\psi_d$. Thus, the adjoint variable p can be calculated and the gradient of J with respect to ϵ can be computed.

Assume that the interval $[0,T]$ has been discretized into a finite number N_{steps} of subintervals of size δt, and $t_m=(m-1)\delta t$. A discrete state variable at t_m is denoted by ψ^m. To obtain a step size that guarantees a uniform decrease in the cost functional, we use the Armijo rule with backtracking [21]. In the sequel we denote by $\tilde{J}(\epsilon):=J(\psi(\epsilon),\epsilon)$, where $\psi(\epsilon)$ is the unique solution of the state equation for given ϵ. Furthermore, we decompose ϵ into its real and imaginary parts, respectively, i.e., $\epsilon=\epsilon_r+i\epsilon_i$. The whole optimal-control (OPC) algorithm is then specified as follows.

(1) Initialize ϵ^{old}, $0<c\ll 1$, $\nu\geqslant 1$, and $\beta>0$.

(2) (a) Solve the state equation $i\dot{\psi}=(H_0+H_{\epsilon^{old}})\psi$ with $\psi(0)=\psi_0$ (marching forward); obtain ψ^{new}. (b) Solve the adjoint equation $i\dot{p}=(H_0^*+H_{\epsilon^{old}})p-q$ with $ip(T)=\psi(T)-\psi_d$ (marching backwards); obtain p^{new}. (c) Determine a search direction

$$\begin{pmatrix} d_r \\ d_i \end{pmatrix} = -G^{-1}\begin{pmatrix} \nabla_r \tilde{J}(\epsilon^{old}) \\ \nabla_i \tilde{J}(\epsilon^{old}) \end{pmatrix},$$

where

$$\nabla_r \tilde{J}(\epsilon^{old}) = \epsilon_r^{old} - \mathrm{Re}\left[p\cdot\left(\frac{\partial H}{\partial \epsilon_r}\psi\right)^*\right]^{new},$$

$$\nabla_i \tilde{J}(\epsilon^{old}) = \epsilon_i^{old} - \mathrm{Re}\left[p\cdot\left(\frac{\partial H}{\partial \epsilon_i}\psi\right)^*\right]^{new}$$

are the gradients for the real and imaginary parts of ϵ, respectively, and G is a positive definite matrix.

(3) Determine a step size t such that

$$\tilde{J}[\epsilon^{old}+t(d_r+id_i)] < \tilde{J}(\epsilon^{old}) + ct\begin{pmatrix} \nabla_r \tilde{J}(\epsilon^{old}) \\ \nabla_i \tilde{J}(\epsilon^{old}) \end{pmatrix}\begin{pmatrix} d_r \\ d_i \end{pmatrix} \qquad (6)$$

holds:

(a) If $t=\beta$ fulfills Eq. (6), set $\beta:=\nu\beta$, $\epsilon^{new}:=\epsilon^{old}+t(d_r+id_i)$, and go to step (2), else (b) $\beta:=\beta/2$, go to step (3a).

Taking in step (2c), the matrix G equal to the identity matrix leads to the usual gradient method, which can happen to converge slowly. Another idea is to use for G an approximation to the Hesse matrix of J with respect to the real and imaginary parts of ϵ, which leads to quasi-Newton methods [21].

To determine the evolution of the state variable and of the adjoint variable, we consider the implicit second-order Crank-Nicholson scheme. The advantage of the Crank-Nicholson scheme is that it is unconditionally stable and it preserves the probability density $|\psi|^2$ in case of a coherent time evolution [18]. For completeness, we give a brief description of the method. Consider the Schrödinger equation (1). Given the numerical solution at time step m, the value of the wave function at the next time step, $m+1$, is obtained solving the following problem for ψ^{m+1}:

$$i\frac{\psi^{m+1}-\psi^m}{\delta t} = \frac{1}{2}H^{m+1}\psi^{m+1} + \frac{1}{2}H^m\psi^m.$$

Thus ψ^{m+1} is given by

$$\psi^{m+1} = \left(I + i\frac{\delta t}{2}H^{m+1}\right)^{-1}\left(I - i\frac{\delta t}{2}H^m\right)\psi^m,$$

where I is the identity in $\mathbb{C}^n$. Notice the dependence H^m from time step due to the presence of the control in H. The operator $[I+i(\delta t/2)H^{m+1}]$ is a $n\times n$ complex matrix that is easily invertible (it can be computed analytically for small values of n). In case of the adjoint equation marching backwards in time, the formulas above hold by inverting the time direction.

Accuracy of the solution obtained by integrating in time using the Crank-Nicholson scheme (or $\theta=1/2$ method) is known, and we therefore report only the main result. Denote with $e^m=\psi(t_m)-\psi^m$, $m=1,\ldots,N_{steps}$, the error at each time step between the continuous solution $\psi(t)$ and its numerical approximation ψ^m. Then, assuming $e^0=0$, there exist constants L and C such that

$$|e^m| \leqslant C\delta t^2\left[\exp\left(L\frac{t_m}{1-L\,\delta t/2}\right)-1\right],$$

where L is a Lipschitz constant and C is proportional to $\sup_{[0,T]}|\psi'''|$.

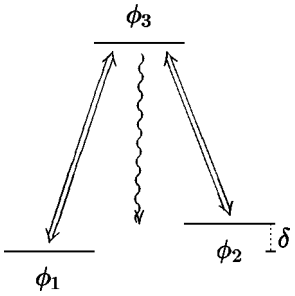

FIG. 1. Prototypical Λ-type level scheme used in our calculations: ϕ_1 and ϕ_2 are long-lived states, whereas ϕ_3 is a short-lived state that is optically coupled to both ϕ_1 and ϕ_2 (for details see text); wiggled line indicates relaxation and dephasing of state ϕ_3.

IV. MODEL SYSTEM

To demonstrate the applicability of our approach, as a first representative example in this paper, we consider the three-level system depicted in Fig. 1, which consists of the following states: two long-lived states ϕ_1 and ϕ_2, which are energetically separated by some amount δ; a state ϕ_3 which has a finite lifetime because of environment coupling (wiggled line). Such Λ-type configurations have a long-standing his-

tory in quantum optics and have been demonstrated successful in the explanation of many coherence phenomena in atomic systems [2,14,22]; more recently, similar configurations have received increasing interest also in semiconductor quantum dots [8,20,23].

Within this scheme, the system's time evolution is governed by the effective Hamiltonian [14,20]

$$H_0=\frac{1}{2}\begin{pmatrix} -\delta & 0 & 0 \\ 0 & \delta & 0 \\ 0 & 0 & -i\gamma_o \end{pmatrix}, \tag{7}$$

where the term $-i\gamma_o$ accounts for the environment losses (e.g., spontaneous photon emissions). Furthermore, the coupling to the external field reads

$$H_\epsilon=-\frac{1}{2}\begin{pmatrix} 0 & 0 & \mu_1\epsilon \\ 0 & 0 & \mu_2\epsilon \\ \mu_1\epsilon^* & \mu_2\epsilon^* & 0 \end{pmatrix}, \tag{8}$$

where μ_1 and μ_2 describe the coupling strengths of states ϕ_1 and ϕ_2 to the interconnecting state ϕ_3 (e.g., optical dipole matrix elements); note that in Eqs. (7) and (8) we have implicitly assumed the usual rotating-wave approximation [2,20]. Initial and final states are then given by

$$\psi_0=\begin{pmatrix} 1 \\ 0 \\ 0 \end{pmatrix}, \quad \psi_d=\begin{pmatrix} 0 \\ e^{-i\delta T} \\ 0 \end{pmatrix},$$

and for the optimality equations (5a) and (5b), we obtain

$$\epsilon=-\frac{1}{2\gamma}\mathrm{Re}[p\cdot(H_1\psi)^*]-i\frac{1}{2\gamma}\mathrm{Re}[p\cdot(H_2\psi)^*],$$

with

$$H_1=\begin{pmatrix} 0 & 0 & \mu_1 \\ 0 & 0 & \mu_2 \\ \mu_1 & \mu_2 & 0 \end{pmatrix}, \quad H_2=\begin{pmatrix} 0 & 0 & i\mu_1 \\ 0 & 0 & i\mu_2 \\ -i\mu_1 & -i\mu_2 & 0 \end{pmatrix}.$$

V. RESULTS

Assuming that the system is initially prepared in state ϕ_1, in the following we address the question: what is the most efficient way to bring the system from ϕ_1 to ϕ_2? Since the direct optical transition between ϕ_1 and ϕ_2 is assumed to be forbidden, we have to use ϕ_3 as an auxiliary state; however, the intermediate population of ϕ_3 introduces losses through environment coupling. Thus, which sequence of laser pulses minimizes the population of level ϕ_3?

A. Simplified model system

To gain insight into the general trends, in the following we shall discuss a somewhat simplified model system (results of our complete calculations will be presented further below). We assume that the three-level system of Fig. 1 is subject to two fields $\epsilon_1(t)=g[t-(t_o/2)]\exp i(\delta/2)t$ and $\epsilon_2(t)=g[t+(t_o/2)]\exp -i(\delta/2)t$, respectively, where $g(t)$ denotes a Gaussian envelope with full width of half maximum τ; in addition, we assume that the first pulse ϵ_1 (centered at time $t_o/2$) only affects the 1-3 transition, and the second pulse ϵ_2 (centered at time $-t_o/2$) only the 2–3 one; such an approximation corresponds to the case that δ is much larger than $\mu_1\epsilon$ and $\mu_2\epsilon$ [2,14].

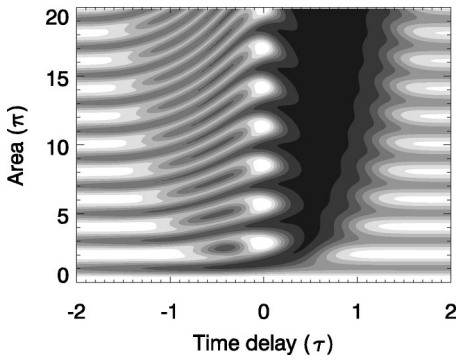

FIG. 2. Results of our calculations for the simplified model system described in the text, and using two laser pulses with Gaussian envelopes (with full width of half maximum τ). Before the pulse sequence the system is in state ϕ_1; black (white) areas correspond to the situation that after the pulse sequence the population of ϕ_2 is one (zero). Negative (positive) time delays correspond to the situation that the ϵ_1 pulse excites the system before (after) the ϵ_2 one, and the pulse area is defined as $\int_{-\infty}^{\infty}dtg(t)$ (we use $\mu_1=\mu_2=1$ and $\gamma_o=0.2\tau^{-1}$).

In Fig. 2, we present results for this simplified model system for different time delays t_o between the two pulses and for different pulse areas (as defined in the figure caption) As regarding the general trends, we observe in Fig. 2 that successful population transfer between the states ϕ_1 and ϕ_2 can be achieved for both negative and positive time delays t_o. In the first case, the pulse ϵ_1 excites the system *before* the ϵ_2 one; here, ϵ_1 brings the system from ϕ_1 to the auxiliary state ϕ_3, and ϵ_2 channels the population between ϕ_3 and the final state ϕ_2; apparently, the efficiency of this transfer, which is known as the stimulated emission pumping technique [14], becomes maximal when the pulse areas are odd multiples of π. In contrast, for positive time delays, i.e., when the ϵ_1 pulse excites the system *after* the ϵ_2 one, the population transfer is not achieved through intermediate shelving of population; for that reason, the sequence of laser pulses is called *counterintuitive*, and the whole process has been given the name stimulated Raman adiabatic passage (STIRAP) [14]. This STIRAP process exploits the renormalizations of quantum states in presence of the strong laser fields, and population transfer is achieved by keeping ψ_3 negligible throughout; see Ref. [14] for an excellent review.

B. Optimal control

We next consider the population transfer for our complete model system of Eqs. (7) and (8), i.e., ϵ affects both the 1-3 and 2-3 transitions, within the framework of *optimal control* (see Ref. [24] for a related optimization analysis of the co-

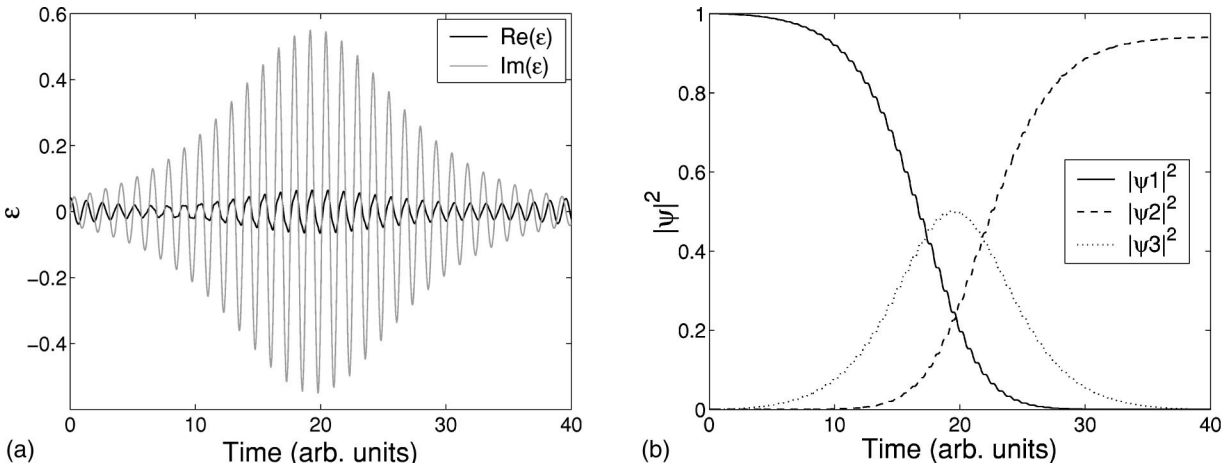

FIG. 3. Results of our optimal-control calculations for $\gamma=0.001$, $\alpha=0$; (a) optimal control and (b) transients of ψ_1, ψ_2, ψ_3.

herent dynamics). As will become apparent from our following discussion, we can change the characteristics of the transfer process between the two limiting cases through different penalizations of ψ_3, i.e., through modification of the weight $\alpha=\alpha_3$ in the cost functional (3). In the solution of Eqs. (5a)–(5c), we use $c=0.001$, $\nu=1.1$, and initialize β with 0.2 (we checked that our results do not depend decisively on these parameters). Furthermore, we use $\mu_1=\mu_2=1$, $\delta=10$, $\gamma_o=0.01$, and consider a final time $T=40$. To update the matrix G in our algorithm we use the Broyden-Fletcher-Goldfarb-Shanno formula [21]. Unless otherwise specified, $\epsilon=0.1\exp(i\delta t)$ for the initialization of the algorithm, and we stop the iteration if the norm of the gradient is less then 10^{-5}.

Figure 3(a) shows results for the control field and Fig. 3(b) for the quantum-state population for $\alpha=0$ (i.e., no penalization of ψ_3). We observe that the population is channeled through occupation of the interconnecting ϕ_3 state, in close resemblance to the stimulated emission pumping process; indeed, analyzing the Fourier transform of the control field [Fig. 3(a)], we find two strong contributions at frequencies $-\delta/2$ and $\delta/2$, where the first one dominates at times below 20 and the latter one in the second half of the transfer process.

Further insight into the pertinent calculation parameters can be obtained from Table I which reports the influence of γ (3), on: the tracking error $|\psi(T)-\psi_d|^2_{C^3}$, i.e., the measure of how accurately the final state is reached; the value of the cost functional J; and the number of iterations of required minimization steps. Quite generally, we observe that allowing stronger field strengths through choice of smaller γ values results in a more efficient population transfer, as one would already expect from the discussion of the simplified model system; here, the increased control field allows for faster $1\rightarrow3$ and $3\rightarrow2$ transitions and, in turn, smaller environment losses due to population of ϕ_3. We also verified that the on and off switching of the control fields can be controlled by replacing ϵ in the state equation by $\xi(t)\epsilon$, where $\xi(t)$ is a function that smoothly approaches zero at early and late times; such an additional control might be required to account for the limited laser resources in the experiment. We finally note that the number of required iterations of the algorithm significantly increases as γ decreases, which we attribute to the increasing singularity of the optimal-control problem as $\gamma\rightarrow0^+$.

TABLE I. Results of our calculations for different values of γ.

γ	$\lvert\psi(T)-\psi_d\rvert^2_{C^3}$	J	Number of iterations
10^{-1}	5.76×10^{-3}	3.93×10^{-2}	26
10^{-2}	2.68×10^{-3}	5.53×10^{-3}	63
10^{-3}	7.44×10^{-4}	1.11×10^{-3}	123
10^{-4}	1.68×10^{-4}	2.44×10^{-4}	360

Finally, in Fig. 4, we show the influence of the penalization of the ϕ_3 population through finite values of α_3 [Eq. (3)] on the solution of the optimal-control problem, which results in a strong reduction of the population-transfer time. From the Fourier transform of the control field of Fig. 4, we furthermore infer that here the time ordering of the two dominant frequency components is reversed as compared to the $\alpha=0$ case, thus making this excitation scenario similar to the STIRAP process.

VI. CONCLUSIONS

In conclusion, we have presented a theoretical analysis of optimal control of quantum nanostructures. A general solution scheme for the optimization of an external control (e.g., lasers pulses) has been developed, which allows to channel the system's wave function between the two given states in its most efficient way; physically motivated constraints, such as limited laser resources or population suppression of certain states, can be accounted for through a general cost functional. A computer algorithm for the solution of the optimal-control problem has been derived and analyzed in detail. Finally, we have demonstrated the applicability of our approach for a generic three-level quantum system, and we have identified the pertinent calculation and convergence parameters.

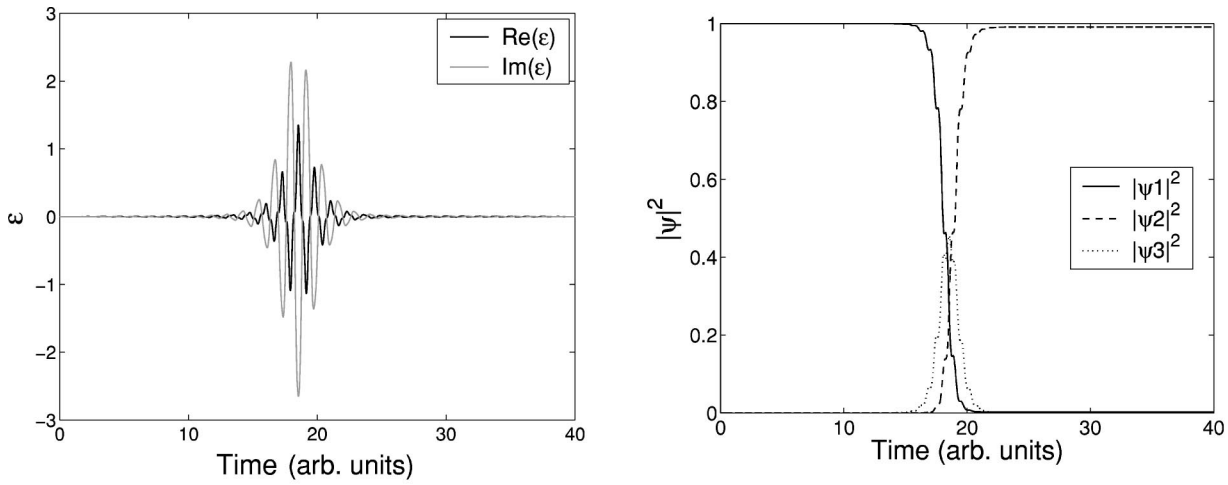

FIG. 4. Same as Fig. 3 but for $\alpha = 0.01$.

Apparently, the true strength of optimal control can only be appreciated in the study of higher-dimensional systems where the control strategies can no longer be grasped from simple considerations, which are needed, e.g., for the design of quantum gates in future quantum registers. There, the high flexibility of our present approach, which solely relies on the state equation and a general functional accounting for the control constraints, renders *optimal control* as an ideal tool for both theoretical modeling as well as experimental support. In this respect, it will be necessary to develop more efficient numerical methods for the solution of the *bilinear* optimal-control problem of our present concern. Future work will also address applications beyond the presently studied three-level scheme.

ACKNOWLEDGMENTS

This work was supported in part by the *Fonds zur Förderung der wissenschaftlichen Forschung* (FWF) under SRC 03 ''Optimization and Control'' and Project No. P15752.

[1] *Coherent Control in Atoms, Molecules, and Semiconductors*, edited by W. Pötz and W.A. Schroeder (Kluwer, Dordrecht, 1999).
[2] M.O. Scully and M.S. Zubairy, *Quantum Optics* (Cambridge University Press, Cambridge, UK, 1997).
[3] H. Rabitz, R. de Vivie-Riedle, M. Motzkus, and K. Kompka, Science **288**, 824 (2000).
[4] A.P. Heberle, J.J. Baumberg, and K. Köhler, Phys. Rev. Lett. **75**, 2598 (1995).
[5] L. Jacak, P. Hawrylak, and A. Wojs, *Quantum Dots* (Springer, Berlin, 1998).
[6] N.H. Bonadeo, J. Erland, D. Gammon, D. Park, D.S. Katzer, and D.G. Steel, Science **282**, 1473 (1998).
[7] T.H. Stievater, X. Li, D.G. Steel, D. Gammon, D.S. Katzer, D. Park, C. Piermarocchi, and L.J. Sham, Phys. Rev. Lett. **87**, 133603 (2001).
[8] U. Hohenester, F. Troiani, E. Molinari, G. Panzarini, and C. Macchiavello, Appl. Phys. Lett. **77**, 1864 (2000).
[9] E. Pazy, I. D'Amico, P. Zanardi, and F. Rossi, Phys. Rev. B **64**, 195320 (2001).
[10] E. Biolatti, R.C. Iotti, P. Zanardi, and F. Rossi, Phys. Rev. Lett. **85**, 5647 (2000).
[11] P. Chen, C. Piermarocchi, and L.J. Sham, Phys. Rev. Lett. **87**, 067401 (2001).
[12] C. Piermarocchi, P. Chen, Y.S. Dale, and L.J. Sham, Phys. Rev. B **65**, 075307 (2002).
[13] *The Physics of Quantum Information*, edited by D. Bouwmeester, A. Ekert, and A. Zeilinger (Springer, Berlin, 2000).
[14] K. Bergmann, H. Theuer, and B.W. Shore, Rev. Mod. Phys. **70**, 1003 (1998).
[15] R.R. Ernst, G. Bodenhausen, and A. Wokaun, *Principles on Nuclear Magnetic Resonance in One and Two Dimensions* (Dover, New York, 1987).
[16] J.L. Lions, *Optimal Control of Systems Governed by Partial Differential Equations* (Springer, Berlin, 1971).
[17] P. Neittaanmäki and D. Tiba, *Optimal Control of Nonlinear Parabolic Systems* (Dekker, New York, 1994).
[18] A.P. Peirce, M.A. Dahleh, and H. Rabitz, Phys. Rev. A **37**, 4950 (1988).
[19] H.O. Fattorini, *Infinite Dimensional Optimisation and Control Theory* (Cambridge University Press, Cambridge, UK, 1999).
[20] U. Hohenester, F. Troiani, and E. Molinari, in *Radiation-Matter Interaction in Confined Systems*, edited by l.C. Andreani, G. Benedek, and E. Molinari (Soc. Italiana di Fisica, Bologna, 2002), p. 25.
[21] D. P. Bertsekas, *Nonlinear Programming* (Athena Scientific, Belmont, 1999).
[22] L. Mandel and E. Wolf, *Optical Coherence and Quantum Optics* (Cambridge University Press, Cambridge, 1995).
[23] T. Brandes and F. Renzoni, Phys. Rev. Lett. **85**, 4148 (2000).
[24] U. Boscain, G. Charlot, J.-P. Gauthier, S. Guérin, and H.-R. Jauslin, J. Math. Phys. **43**, 2107 (2002).